

## Compact Electronic Gamma Source for Radiotherapy

A. X. Chen<sup>a,b</sup>, A. J. Antolak<sup>a</sup>, K. -N. Leung<sup>c</sup>, T. N. Raber<sup>a</sup>, D. H. Morse<sup>a</sup>

<sup>a</sup>Sandia National Laboratories, PO Box 969, Livermore, CA, 94550

<sup>b</sup>Department of Mechanical Engineering, University of California, Berkeley, CA 94720

<sup>c</sup>Department of Nuclear Engineering, University of California, Berkeley, CA 94720

6

7 **Abstract.** A compact mono-energetic gamma source is being developed to replace the radiological sources used in  
8 radiotherapy and other medical instruments. The electronic gamma source utilizes low energy nuclear reactions to  
9 generate primary gammas in the 0.5 to 1.0 MeV energy range. Deuterium ions are injected from an RF-driven ion  
10 source into a pyroelectric crystal-based acceleration system, allowing independent control of the current and energy  
11 of the  $D^+$  ion beam. The  $D^+$  ions are accelerated to above 100 keV voltages and then bombard a target to produce  
12 gammas. Thermal management of the pyroelectric crystal-based accelerator is achieved by convective dielectric  
13 fluid flow around the crystal. This approach provides better temperature uniformity in the crystal and higher  
14 dielectric strength for suppressing voltage breakdown and enabling faster thermal cycling rates.

15

16 **Keywords:** LiTaO<sub>3</sub> pyroelectric crystal accelerator, gamma generator, 13.56 MHz RF ion source, <sup>9</sup>Be(D,ng)<sup>10</sup>B  
17 nuclear reaction, radiotherapy, dielectric fluid

18 PACS: 29.25.Dx; 29.25.Dz; 77.70.+a

## INTRODUCTION

According to the National Cancer Institute, half of all men and one third of all women will develop some form of cancer during their lifetime (1). Radiotherapy has proved to be an effective non-surgical treatment against many kinds of tumors. In particular, gamma--based radiotherapy gives physicians unparalleled control of the dose delivery depth to allow precise attacks on tumor cells while preserving healthy cells. Current radiotherapy instruments such as gamma knives use an array of radioactive sources which are collimated onto a single point (tumor) for irradiation treatments (2). Recently, however, national security issues regarding the use of high activity

1 radiological sources in medical and commercial applications have been raised (3). As a result, there is increased  
 2 interest in developing electronic sources to replace the existing radiological sources since they can be turned off  
 3 when not in use and can be designed to produce gammas with energies similar to existing instruments. In particular,  
 4 the development of an electronic mono-energetic gamma source producing gammas in the range of 0.5 - 1 MeV  
 5 would be a good replacement for the  $^{60}\text{Co}$ ,  $^{137}\text{Cs}$ , or  $^{192}\text{Ir}$  sources currently used in radiotherapy.

## 6 GAMMA SOURCE CONCEPT

7 The gamma source concept is based on using low energy nuclear reactions to produce the desired radiation  
 8 by extracting a beam from a suitable ion source and accelerating it across a single gap onto a production target. A  
 9 deuterium beam impinging on a  $^9\text{Be}$  target will generate gammas with energies 410 keV, 718 keV, 1.03 MeV, 1.44  
 10 MeV, and 2.87 MeV, with the 718 keV and 1.03 MeV gammas having the highest emission probabilities (4). The  
 11  $^9\text{Be}(\text{D},\text{n}\gamma)^{10}\text{B}$  reaction cross section (FIGURE 1) shows a general increasing logarithmic behavior from  
 12 approximately 100 keV up to 700 keV. While the magnitude of the cross section continues to increase with  
 13 increasing deuteron energy, the rate of increase is slower above  $\sim$ 300 keV (see Figure 1), so the present gamma  
 14 source is designed to operate around 300-400 keV.

15 In the present system, the gamma source employs a pyroelectric crystal powering system to achieve the  
 16 required voltage for optimum gamma production in a compact device. A non-zero spontaneous polarization  
 17 develops across the crystal in the pyroelectric effect due to a change in the crystal temperature, resulting in a charge  
 18 on its polar face given by

$$19 Q = \gamma A \Delta T \quad [1]$$

20 where  $Q$  is the net charge,  $\gamma$  is the pyroelectric coefficient,  $A$  is the area of the crystal polar face, and  $\Delta T$  is the  
 21 temperature change (5). The voltage is given by:

$$22 V = \frac{\gamma A \Delta T}{C} \quad [2]$$

23 where  $C$  is the capacitance of the system. It is important to note that the voltage may not be constant over time due  
 24 to the functional dependence between the ion current load on the crystal and the rate of temperature change.  
 25 Differentiating [1] with respect to time gives the relationship between the current and rate of temperature change,

$$26 I_a = \frac{dQ}{dt} = \gamma A \frac{dT}{dt} \quad [3]$$

1 where  $I_a$  is the available current. Assuming negligible losses, the voltage can be kept constant if  $I_a = I_{load}$  by  
2 controlling  $I_{load}$  through a separate ion source.

### 3 GAMMA SOURCE DESIGN

4 The prototype gamma source in [FIGURE 2](#) consists of three major components: 1) RF ion source, 2)  
5 pyroelectric crystal acceleration system, and 3) gamma production target. In the prototype, a 10" diameter stainless  
6 steel chamber is used to house the crystal accelerator and gamma production target. The ion source is mounted on a  
7 6" Conflat flange attached to the chamber. A turbo-molecular pump coupled with a roughing vacuum pump is used  
8 to provide vacuum for the chamber and ion source. A needling valve is used to adjust the pressure for the ion source.  
9 The ion source and acceleration regions are separated to allow differential pumping to the desired pressure for  
10 optimal ion source plasma operation while the pyroelectric accelerator chamber can be pumped to a pressure several  
11 orders of magnitude lower to generate higher voltages and minimize arc discharges. Tests made with a 1 mm  
12 diameter aperture showed that the pyroelectric accelerator chamber pressure can be maintained in the  $10^{-5}$  Torr range  
13 while the plasma chamber is operating in the  $10^{-2}$  Torr range. Additionally, the current load on the pyroelectric  
14 crystal accelerator can be varied by changing the ion source parameters, allowing independent control of the  
15 accelerator current and voltage.

16 The prototype gamma source design implements an RF discharge plasma ion source to produce the  
17 deuterium ( $D^+$ ) ion beam (6). Mass spectrometer measurements of the hydrogen species fractions in the RF  
18 discharge ion source show a high ratio of atomic compared to molecular ions ([FIGURE 3](#)). This is ideal for the  
19 gamma source because  $D^+$  ions will achieve the full potential energy from the pyroelectric crystal accelerator, while  
20  $D_2^+$  and  $D_3^+$  will produce deuterium ions with 1/2 and 1/3 of the full energy, respectively, resulting in lower gamma  
21 yield.

22 During operation of the ion source, a 13.56 MHz RF field is coupled to a quartz chamber that is  
23 continuously filled with deuterium gas regulated to a pressure of 10-50 mTorr. A circular array of Nd-Fe-B magnets  
24 is placed around the chamber for better plasma confinement. Ceramic standoffs are used to separate the extraction  
25 electrode from the ion source. Deuterium ions are extracted with low (0.1-1.0 kV) extraction voltage and low (5-20  
26 W) RF power. The available ion current,  $I_a$ , depends on several parameters including extraction voltage, RF power,  
27 and plasma density (7). The ion source current was measured with a Faraday cup placed at the target location

1 (FIGURE 3). Measurements indicated that the current is in the range of 0.1 to 10's of nano-amperes for the above  
2 described conditions.

3 The D<sup>+</sup> ions are extracted from the ion source and accelerated to high energies (>100 keV) using the  
4 pyroelectric crystal. The acceleration system is comprised of a 10 cm long x 1 cm diameter LiTaO<sub>3</sub> crystal housed  
5 in a polythermide tube as shown in FIGURE 4. The use of a long crystal reduces the electric field gradient of the  
6 accelerator system, providing better voltage holding and stability of operation. Using Equations 1 and 2 above, the  
7 theoretically surface charge and voltage for a LiTaO<sub>3</sub> crystal of these dimensions are ~15 nC and 48.8 keV per  
8 degree Celsius of temperature change. Heating and cooling of the crystal is provided by continuous flow of a  
9 dielectric fluid (Fluorinert<sup>TM</sup> FC-70) around the entire crystal. One end of the crystal polar face is grounded via a  
10 metal spring structure connected to the vacuum chamber, while the other end is electrically connected to a sealing  
11 screw which protrudes out of the assembly for attachment of the gamma production target. The entire accelerator  
12 system is flanged inside the 10" vacuum chamber through an Ultra-Torr<sup>®</sup> adapter.

13 Electrostatics modeling of the pyroelectric accelerator system and gamma production target based on  
14 Equation 1 and the specific geometry predicts that -300 kV can be achieved with a temperature change of  
15 approximately 150°C. During operation, a heated reservoir of dielectric fluid is pumped into the polythermide tube,  
16 heating the crystal and generating the necessary voltage for the D-Be nuclear reaction. The system temperature is  
17 monitored with thermocouples placed in the fluid reservoir and at the grounded end of the pyroelectric crystal. A  
18 LabVIEW<sup>TM</sup> program is used to control the flow rate and reservoir temperature giving the desired transient fluid  
19 temperature profile which depends on the bath temperature, thermal capacitance of the fluid hardware and crystal  
20 assembly, and flow rate of the fluid. The temperature profile of the crystal can be modeled as a one-dimensional  
21 transient conduction problem with convective and insulated boundary conditions (8). Because of the uniform fluid  
22 bath surrounding the crystal, the effective thermal length is the radius (5 mm) of the crystal. A thermal penetration  
23 depth analysis shows only a few degrees difference between the center and surface of the crystal during a moderate  
24 temperature ramp of 2 °C/s.

25 A separate fluid loop is connected to the pyroelectric accelerator to provide cold dielectric fluid into the  
26 system and return the crystal to ambient temperature. The convective heating scheme using dielectric fluid provides  
27 better temperature uniformity throughout the crystal compared to only heating it from one end.

1 A 0.010" thick beryllium foil is used for the gamma production target. The foil is attached to a 1.18"  
2 diameter x 0.5" long hollow aluminum cylinder fastened to the sealing screw protruding from the pyroelectric  
3 crystal. A pair of magnets are attached to the inside of the cylinder to suppress back streaming electrons when  $D^+$   
4 ions impinge the target.

## EXPERIMENTAL RESULTS

6 The ion source was initially operated with argon plasma to measure the voltage produced by the  
7 pyroelectric crystal and calibrate the detectors. In this case,  $\text{Ar}^+$  ions were accelerated onto a target and produced  
8 back streaming electrons at energy equal to the pyroelectric crystal voltage. The electron energy was measured by a  
9 Si surface barrier detector mounted inside the chamber with line of sight on the incident face of the target. The  
10 surface barrier detector was initially calibrated using a metal target biased to -70 kV in place of the pyroelectric  
11 accelerator and target assembly. The resulting electron energy spectra from the  $\text{Ar}^+$  ion bombardment of the metal  
12 target showed the main peak corresponding to the bias voltage and subsequent peaks caused by pileup in the surface  
13 barrier detector. The pileup can be reduced by using a very small extraction aperture to reduce the electron intensity.  
14 A 5" x 5" NaI detector was also externally mounted near the chamber viewport to measure the X-ray endpoint  
15 energy of the back streaming electrons as they strike the chamber wall. Unfortunately, no X-rays were measured by  
16 the NaI detector due to the very low signal-to-noise ratio.

17 The NaI detector was initially calibrated with a  $^{137}\text{Cs}$  source and a background measurement was made near  
18 the gamma source. In this first generation system, the D-Be gammas are only produced during the heating phase in  
19 which the beryllium target becomes negatively charged. The crystal was heated rapidly from approximately 30°C  
20 to 90°C in 20 seconds by pumping the hot dielectric fluid into the pyroelectric system. Additional experiments to  
21 quantify the voltage, characterize the gamma spectrum, and improve device performance are in progress.

## CONCLUSION

23 A prototype electronic gamma source has been built and preliminary operational tests performed. The  
24 source utilizes a pyroelectric crystal to accelerate  $D^+$  ions onto a beryllium reaction target to produce gamma-rays in  
25 the 0.5-1.0 MeV energy range. Thermal management of the pyroelectric accelerator is achieved by convective flow  
26 of a dielectric fluid around the entire crystal providing better temperature uniformity in the crystal, suppression of

1 voltage breakdowns between the crystal polar faces, and faster thermal cycling rates. Operational tests indicate that  
2 improved performance could be attained by synchronizing the RF power with the ion beam extraction pulse and by  
3 improving the target geometry. For example, a torus-like geometry could give lower potential gradients in the  
4 vicinity of the target and reduce the secondary electron emission from the target.

5 **ACKNOWLEDGEMENT**

6 The author would like to thank Professor Ralph Greif and Samuel S. Mao for useful discussion of the  
7 experiment. This work was funded by DOE/NA-22 Office of Nonproliferation Research and Development. Sandia  
8 National Laboratories is a multi-program laboratory operated by Sandia Corporation, a wholly owned subsidiary of  
9 Lockheed Martin Company, for the U.S. Department of Energy's National Nuclear Security Administration under  
10 contract DE-AC04-94AL85000.

11 **REFERENCES**

12 1. American Cancer Society (<http://www.cancer.org/Cancer/CancerBasics/lifetime-probability-of-developing-or-dying-from-cancer>).

14 2. <http://www.gammaknife.com>.

15 3. Findings of the President of the Conference, Proceedings of the International Conference on Security of  
16 Radioactive Sources, Vienna, Austria, IAEA, (2003).

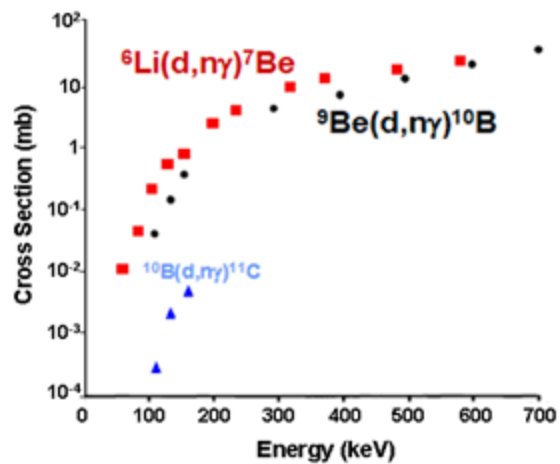
17 4. F.E. Cecil, R. F. Fahlsing and R. A. Nelson, Nuc. Phys. 376, 379-388 (1982).

18 5. A.M. Glass Phys. Rev. Vol. 172, Issue 2 pp. 564-571 (1968).

19 6. Y. Wu, J.P. Hurley, Q. Ji, J. Kwan, K.N. Leung, AIP Conf. Proc. Vol. 1099, Issue 1 pp. 614-618 (2009).

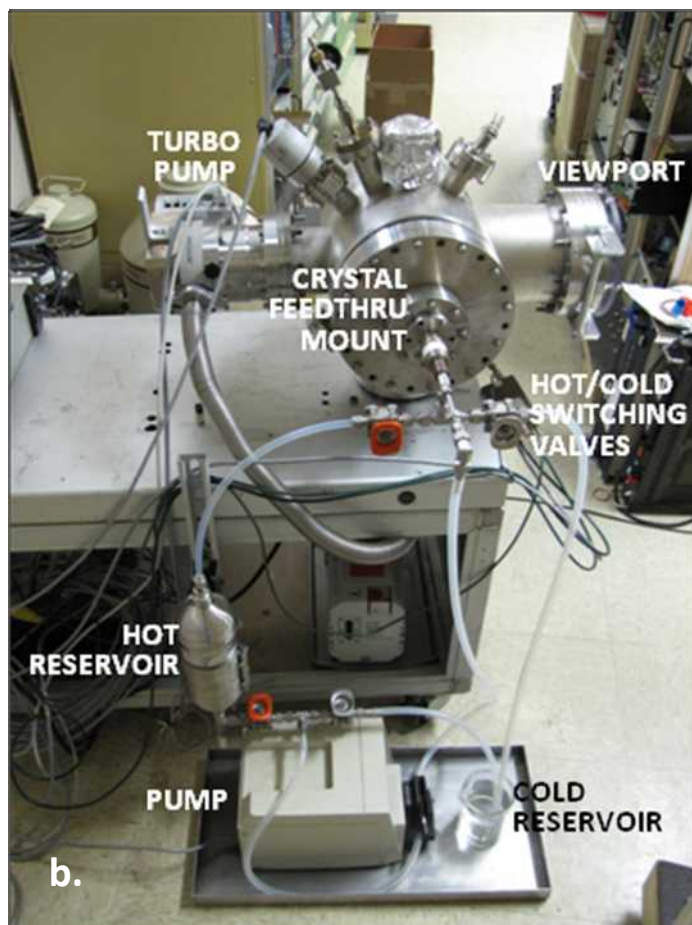
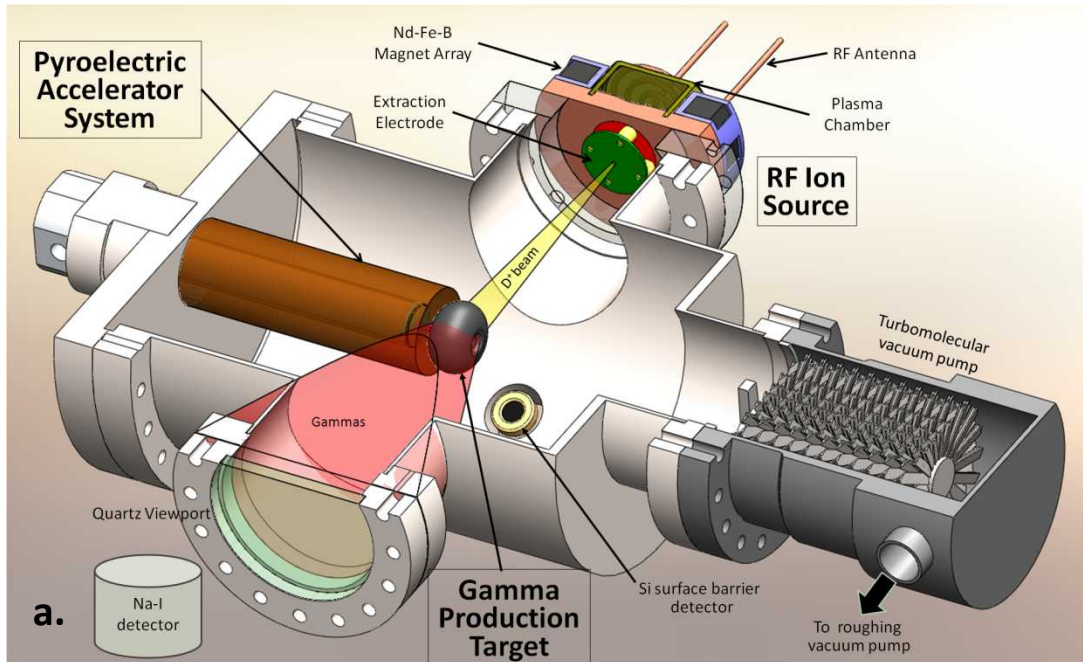
20 7. X. Jiang, Q. Ji, A. Chang, K.N. Leung, Rev. of Sci. Instr. Vol. 74, Issue 4 pp. 2288-2293(2003).

21 8. F.P. Incropera, D.P. DeWitt, "Transient Conduction," in *Fundamentals of Heat and Mass Transfer*, New York,  
22 John Wiley and Sons, 2002, pp. 254-260 .

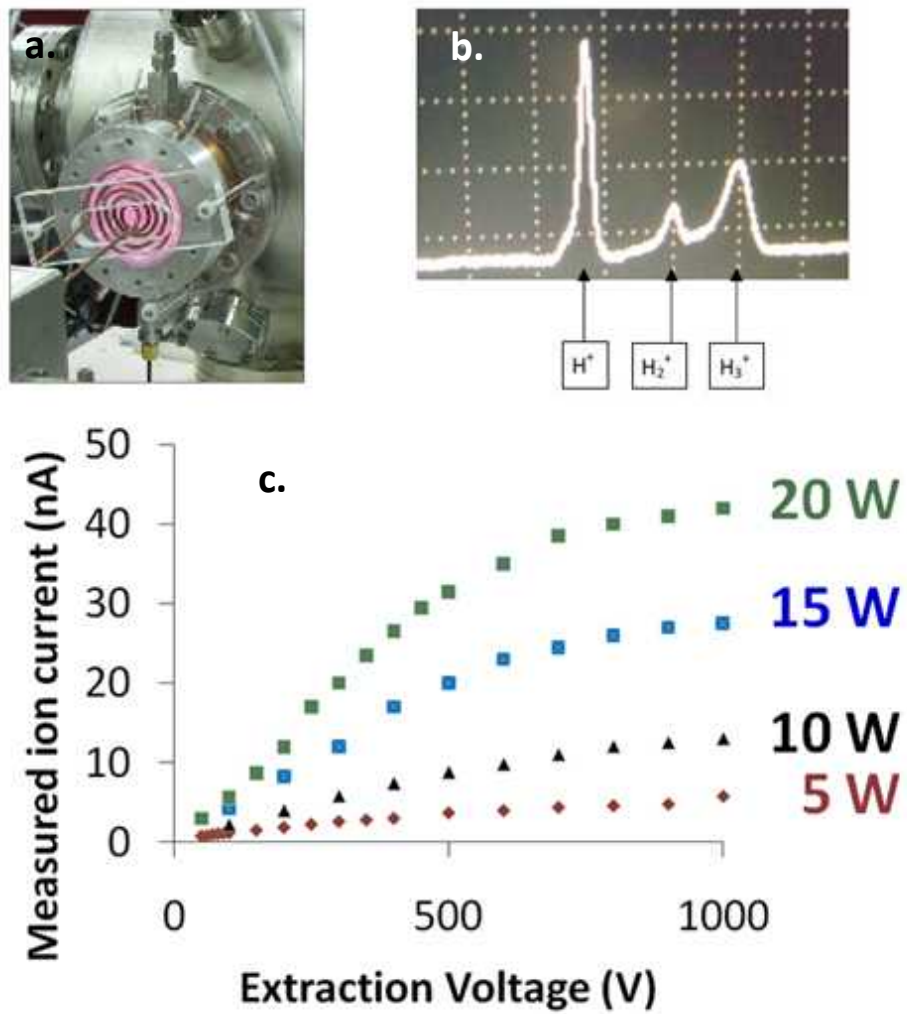


1

2 **FIGURE 1.** Reaction cross-sections of several nuclear reactions for gamma production (from Ref. 4).

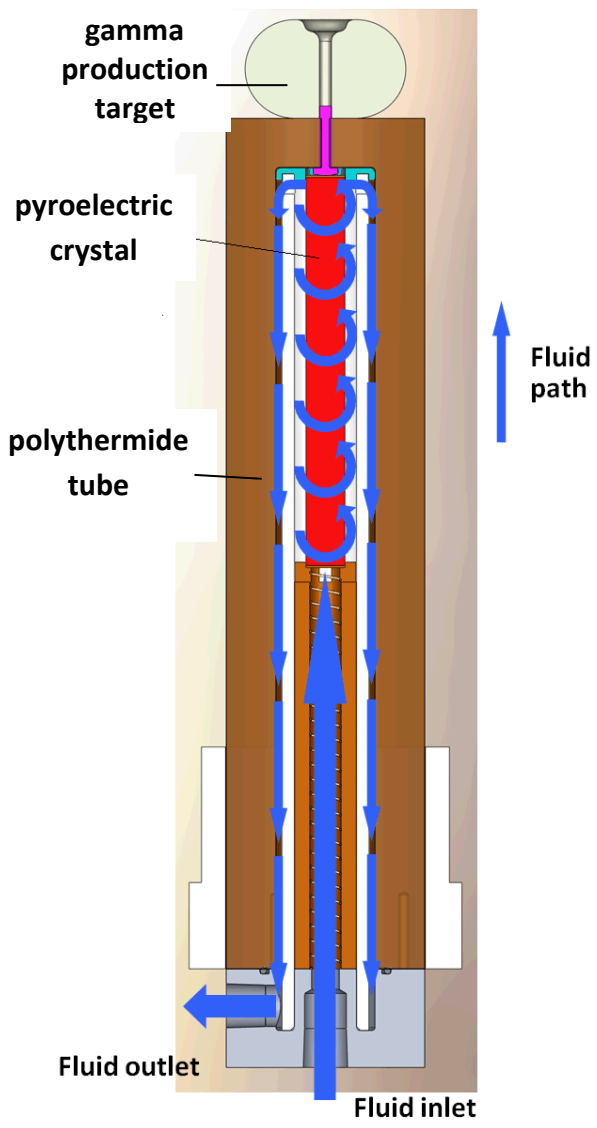


3 **FIGURE 2.** a) CAD model and b) photo of the prototype gamma source with dielectric fluid heating system.



1

2 **FIGURE 3.** a) RF discharge ion source, b) mass spectrum of the hydrogen plasma, and c) ion source current as a  
3 function of extraction voltage and RF power.



1

2 **FIGURE 4.** Cross-sectional schematic of the pyroelectric crystal acceleration system.